Taylor & Francis
Taylor & Francis Group

Automatika

Journal for Control, Measurement, Electronics, Computing and Communications

ISSN: (Print) (Online) Journal homepage: www.tandfonline.com/journals/taut20

A high efficient 33 level inverter for electric vehicle application using PMSM

N. Subha Lakshmi & S. Allirani

To cite this article: N. Subha Lakshmi & S. Allirani (2024) A high efficient 33 level inverter for electric vehicle application using PMSM, Automatika, 65:3, 706-715, DOI: 10.1080/00051144.2024.2309445

To link to this article: https://doi.org/10.1080/00051144.2024.2309445

Published online: 19 Feb 2024.

AUTOMATIKA
2024, VOL. 65, NO. 3, 706–715
https://doi.org/10.1080/00051144.2024.2309445

A high efficient 33 level inverter for electric vehicle application using PMSM

N. Subha Lakshmi [a] and S. Allirani[b]

[a]Department of EEE, Sri Krishna College of Engineering and Technology, Coimbatore, India; [b]Department of EEE, Sri Ramakrishna Engineering College, Coimbatore, India

ABSTRACT

The permanent magnet synchronous motor (PMSM) avoids commutation-related torque ripples and produces smooth torque. Its great handling capacity and better efficiency make it an excellent choice for high-demand applications. A typical PM motor drive fed with pulse width-modulated voltages may cause the motor insulation to break down if rapid voltages (dv/dt) occur across the motor terminals. Applying variable voltage with low dv/dt and implementing multiple inverter topology can solve this issue. Multilevel converters have minimal switching losses, better power quality and the ability to operate at both fundamental and higher switching frequencies. In this study, a three phase stacked multilevel inverter-based FOC driven PMSM drive design is proposed. Here, the neutral point is a capacitor intermediate point on DC side, where current is naturally balanced throughout a switching cycle. This makes it possible to use downstream batteries and even lower voltage equipment, greatly increasing efficiency, improved performance and smother control at low speed. Therefore, direct-battery-driven electric vehicles will be able to use this. A 33 level inverter-based PMSM drive was used to implement the FOC, and the simulation results were used to validate it. The Matlab/Simulink tool is used to simulate the entire system.

ARTICLE HISTORY
Received 5 September 2023
Accepted 18 January 2024

KEYWORDS
PMSM (permanent magnet synchronizer); multilevel converter; FOC (Field Oriented Controller); Pulse Width Modulation (PWM)

1. Introduction

More focus has been placed on electric vehicles (EVs) as a potential solution to the crisis of energy and ecological concerns [1,25]. The prevalence of EVs will rise rapidly in the upcoming years due to research activities and ongoing advancements in control strategies and electrical drive systems [2]. The drive train, power converter, and electric machine make up an EV's electrical driving system [3]. Presently, EVs can be powered by a wide range of electrical drive technologies, including two- or multi-level power converters and induction motors (IM) or permanent magnet synchronous motors (PMSM). With regard to the electric machine component, PMSMs are thought to be viable options for EV applications due to their potential for low maintenance, a simpler control scheme, reliable operations, high efficiency, and high energy density [4]. In EV applications, two-level inverters are typically utilized to regulate the PMSM [5]. Multilevel converters can function at a high rate of switching PWM in addition to fundamental switching frequency. A power-electronic device known as a multilevel inverter uses several PWM algorithms to produce the desired output voltage.

Since multilevel inverters (MLI) use switches with lesser voltage ratings, offer superior quality waveform even at lower switching frequencies, have fewer electromagnetic issues with compatibility and, require less filtering, they are a logical choice for high power inverter drives [6]. cascaded Hbridge Inverter, flying capacitor MLC, Diode clamped inverters, and MLC hybrid topologies are examples of typical multilevel converter (MLC) topologies [7]. Research into producing more voltage levels has been extensive since it has been shown that minimize harmonic content in the waveform [8]. When increasing the number of voltage level, diode clamped inverter necessitate a high quantity of DC link balancing capacitors, and clamping power diodes also becomes more challenging. Large numbers of electrolytic capacitors are needed for FCs, and balancing these flying capacitors is increasingly difficult as the voltage waveform climbs up. Despite their modular design, the CHBs need more separate DC supplies to function. There have been numerous reports of hybrid topologies with voltage waveforms that contain additional steps.

In [9,10], the management and functioning of a 7-level inverter are covered in great detail. In [11], a 9-level open-ended setup for induction motor drives is covered. To balance out the loss distribution across semiconductor switches, Active NPCs were introduced [12]. Another type of MLC that can produce increased voltage level waveforms is the hybrid MLC, which is

CONTACT N. Subha Lakshmi nsubhalakshmi90@gmail.com Department of EEE, Sri Krishna College of Engineering and Technology, Coimbatore, Tamil Nadu, India

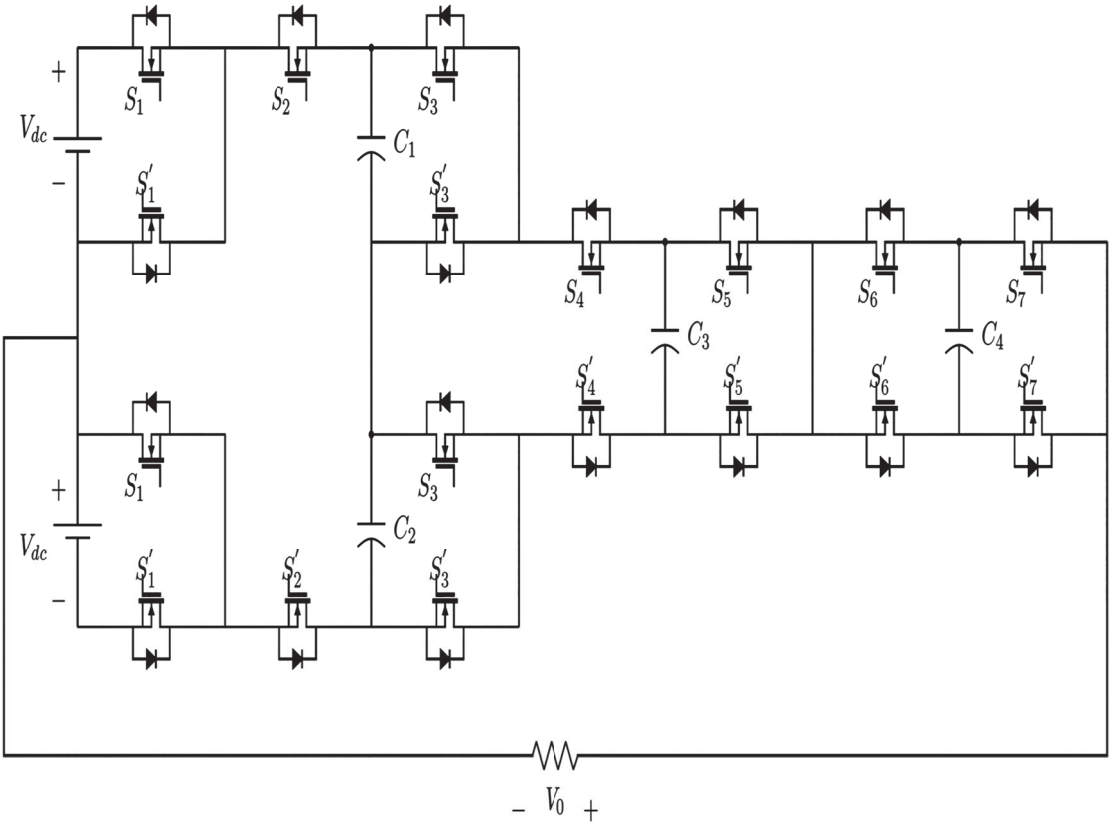

Figure 1. Proposed 33-level stacked circuit diagram of MLIs.

created by combining FCs and several CHBs. Literature reports on hybrid converters with a single DC supply for 5-level and 17-level [13]. The investigation of neutral point (NP) oscillations in multiphase NPCs [15] and three phase NPCs [14] has been documented in a number of articles. A thorough examination of the impact of nonlinearities on the neutral point can be found in [16]. In [17], the analysis and management of DC capacitor voltage drift in a 5-level inverter are covered. A new report [18] for three phase IM drives describes another way to create increased voltage level waveforms by layering MLCs with reduced space vector structure and using low voltage devices. The subsequent section replicates the different noteworthy characteristics of these stacked inverters. With instantaneous neutral point (NP) current balancing inside a switching cycle, the stacked inverter topology is utilized in this research to power FOC-based PMSM drives that have just one DC source.

Field Oriented Control, or FOC, is a popular closed-loop control technique that produces PMSMs with remarkable dynamic performance. By separating the components of stator current that produce torque and flux, it makes it possible to regulate the PMSM drive in a decoupled manner, simulating the control structure of a DC machine that is excited independently [23]. Due to its ability to independently adjust torque and flux, FOC effectively converts the control of an alternating current machine into that of a DC machine. In addition to providing an efficient performance across a larger speed range, FOC gives the PMSM full motor torque capabilities at speed ranges below rated speed. The following section lists a few of these stacked inverters' noteworthy characteristics. This paper focuses on instantaneous neutral point (NP) current balancing for FOC-based PMSM drives with a single DC source employing a stacked inverter design.

2. Topology of the proposed stacked multilevel Inverter

Figure 1 Illustrates the proposed 33 level Stacked MLI multilevel inverter, which consists of 18 power switches and 4 capacitors. The suggested 33 level Stacked MLI switching Table 1 is displayed in the table, and the proposed Stacked MLI capacitor can be charged and discharged at the same cycle level. I.

The capacitor voltage $V_{C1}, V_{C2}, V_{C3}, V_{C4}, V_{C5}$ and V_{C6} is specified below.

$$V_{C1} = V_{C2} = 16V_{dc}$$
$$\grave{V}_{C3} = V_{C4} = 4V_{dc}$$
$$V_{C5} = 2V_{dc}$$
$$V_{C6} = V_{dc}$$

The voltage control regulates the charging and discharging of each capacitor to the required voltage level

Table 1. List of on switching states for the proposed 33-level stacked MLIs.

S1	S2	S3	S4	S5	S6	S7	C1	C2	C3	C4	V_{INV}	S1	S2	S3	S4	S5	S6	S7	C1	C2	C3	C4	V_{INV}
1	1	1	1	1	0	0	U	U	U	U	$+16V_{dc}$	0	1	1	1	1	0	0	U	U	U	U	0
1	1	1	1	1	1	0	U	U	U	C	$+15V_{dc}$	0	1	1	1	1	1	0	U	U	U	C	$-V_{dc}$
1	1	1	1	0	0	1	U	U	C	D	$+15V_{dc}$	0	1	1	1	0	0	1	U	U	C	D	$-V_{dc}$
1	1	1	0	1	0	1	C	U	D	D	$+15V_{dc}$	0	1	1	0	1	0	1	C	U	D	D	$-V_{dc}$
1	1	1	1	0	0	0	U	U	C	U	$+14V_{dc}$	0	1	1	1	0	0	0	U	U	C	U	$-2V_{dc}$
1	1	1	0	1	0	0	C	U	D	U	$+14V_{dc}$	0	1	1	0	1	0	0	C	U	D	U	$-2V_{dc}$
1	1	1	1	0	1	0	U	U	C	C	$+13V_{dc}$	0	1	1	1	0	1	0	U	U	C	C	$-3V_{dc}$
1	1	1	0	1	1	0	C	U	D	C	$+13V_{dc}$	0	1	1	0	1	1	0	C	U	D	C	$-3V_{dc}$
1	1	0	1	1	0	1	C	U	U	D	$+13V_{dc}$	0	1	0	1	1	0	1	C	U	U	D	$-3V_{dc}$
1	1	0	1	1	0	0	C	U	U	U	$+12V_{dc}$	0	1	0	1	1	0	0	C	U	U	U	$-4V_{dc}$
1	1	0	1	1	1	0	C	U	U	C	$+11V_{dc}$	0	1	0	1	1	1	0	C	U	U	C	$-5V_{dc}$
1	1	0	1	0	0	1	C	U	C	D	$+11V_{dc}$	0	1	0	1	0	0	1	C	U	C	D	$-5V_{dc}$
1	1	0	0	1	0	1	C	C	D	D	$+11V_{dc}$	0	1	0	0	1	0	1	C	C	D	D	$-5V_{dc}$
1	1	0	1	0	0	0	C	U	C	U	$+10V_{dc}$	0	1	0	1	0	0	0	C	U	C	U	$-6V_{dc}$
1	1	0	0	1	0	0	C	C	D	U	$+10V_{dc}$	0	1	0	0	1	0	0	C	C	D	U	$-6V_{dc}$
1	1	0	1	0	1	0	C	U	C	C	$+9V_{dc}$	0	1	0	1	0	1	0	C	U	C	C	$-7V_{dc}$
1	1	0	0	1	1	0	C	C	D	C	$+9V_{dc}$	0	1	0	0	1	1	0	C	C	D	C	$-7V_{dc}$
1	0	1	1	1	0	1	D	D	U	D	$+9V_{dc}$	0	0	1	1	1	0	1	D	D	U	D	$-7V_{dc}$
1	0	1	1	1	0	0	D	D	U	U	$+8V_{dc}$	0	0	1	1	1	0	0	D	D	U	U	$-8V_{dc}$
1	0	1	1	1	1	0	D	D	U	C	$+8V_{dc}$	0	0	1	1	1	1	0	D	D	U	C	$-9V_{dc}$
1	0	1	1	0	0	1	D	D	U	D	$+7V_{dc}$	0	0	1	1	0	0	1	D	D	U	D	$-9V_{dc}$
1	0	1	0	1	0	1	U	D	D	D	$+7V_{dc}$	0	0	1	0	1	0	1	U	D	D	D	$-9V_{dc}$
1	0	1	1	0	0	0	D	D	C	U	$+6V_{dc}$	0	0	1	1	0	0	0	D	D	C	U	$-10V_{dc}$
1	0	1	0	1	0	0	U	D	D	U	$+6V_{dc}$	0	0	1	0	1	0	0	U	D	D	U	$-10V_{dc}$
1	0	1	1	0	1	0	D	D	C	C	$+5V_{dc}$	0	0	1	1	0	1	0	D	D	C	C	$-11V_{dc}$
1	0	1	0	1	1	0	U	D	U	C	$+5V_{dc}$	0	0	1	0	1	1	0	U	D	U	C	$-11V_{dc}$
1	0	0	1	1	0	1	U	D	U	D	$+5V_{dc}$	0	0	0	1	1	0	1	U	D	U	D	$-11V_{dc}$
1	0	0	1	1	0	0	U	D	U	U	$+4V_{dc}$	0	0	0	1	1	0	0	U	D	U	U	$-12V_{dc}$
1	0	0	1	1	1	0	U	D	U	C	$+3V_{dc}$	0	0	0	1	1	1	0	U	D	U	C	$-13V_{dc}$
1	0	0	1	0	0	1	U	D	C	D	$+3V_{dc}$	0	0	0	1	0	0	1	U	D	C	D	$-13V_{dc}$
1	0	0	0	1	0	1	U	U	D	D	$+3V_{dc}$	0	0	0	0	1	0	1	U	U	D	D	$-13V_{dc}$
1	0	0	1	0	0	0	U	D	C	U	$+2V_{dc}$	0	0	0	1	0	0	0	U	D	C	U	$-14V_{dc}$
1	0	0	0	1	0	0	U	U	D	U	$+2V_{dc}$	0	0	0	0	1	0	0	U	U	D	U	$-14V_{dc}$
1	0	0	1	0	1	0	U	D	C	C	$+V_{dc}$	0	0	0	1	0	1	0	U	D	C	C	$-15V_{dc}$
1	0	0	0	1	1	0	U	U	D	C	$+V_{dc}$	0	0	0	0	1	1	0	U	U	C	D	$-15V_{dc}$
1	0	0	0	0	0	1	U	U	U	D	$+V_{dc}$	0	0	0	0	0	0	1	U	U	U	C	$-15V_{dc}$
1	0	0	0	0	0	0	U	U	U	U	0	0	0	0	0	0	0	0	U	U	U	U	$-16V_{dc}$

Table 2. Topology comparisons of the proposed stacked mlis with existing topologies.

LI Topology	LEVEL	SWITCH	DIODE	DC SOURCE	Capacitor
CHBMLI	33	64	-	16	-
Proposed CHBMLI [9]	33	64	-	32	-
ST-Type[8]	33	24	24	8	-
CSD [10]	33	21		16	
HCMLI [11]	33	34	-	16	-
SBSU STACKED MLIs [21]	33	79	-	1	15
SU STACKED MLIs [20]	33	21	32	1	16
Proposed STACKED MLI	33	18	18	1	6

of each capacitor. The switch can produce both positive and negative voltage levels when it is in the ON and OFF states, respectively.

Table 2 analyzes the number of switches, diode, capacitor, and DC sources for a single phase inverter as a function of 33 voltage levels. The topology of [8], [9], [10], and [11] is not as good as that of the typical CHBMLI, requiring the same number of switches but more DC sources than Stacked MLI, which only requires one DC source. SBSU-Stacked MLI [20] and Stacked MLI SU-StackedMLI [19]. On the other hand, the suggested Stacked MLI requires a notably smaller number of switches and DC sources while requiring the same amount of DC sources as the traditional CHBMLI and Stacked MLI. Consequently, the suggested HCMLI can be used with both single- and three-phase inverters.

3. PMSM mathematical model

In an attempt to simplify the mathematical model of the synchronistic coordinate system of PMSM, the following assumptions are commonly made: ignoring the motor's core saturation, removing the hysteresis and eddy current losses, and maintaining the three phase AC wave current symmetrical; ignoring magnetic saturation with iron loss, magnetic field circuit is maintained linearly, and relying on the inverter to produce absolute three phase power while ignoring the friction in rotor shaft and superior harmonics [24]. Coordinate transformation theory serves as the foundation for the control technique known as vector control. Through the use of coordinate transformation, speed control in PMSM can achieve performance comparable to that of DC motors. In order to achieve this, the flux, motion and torque derivations for the PMSM's model mathematically in the coordinate d-q system can be explained as follows.

Voltage derivation:

$$u_d = R.I_{sd} + P\varphi_{\mathrm{sd}} - \omega.\varphi_{\mathrm{sq}} \tag{1}$$

$$u_q = R.I_{sq} + P\varphi_{\mathrm{sq}} + \omega.\varphi_{\mathrm{sd}} \tag{2}$$

Flux derivation:

$$\varphi_{\mathrm{d}} = \mathrm{L_{sd}}.\mathrm{I_{sd}} + \varphi_{\mathrm{f}} \tag{3}$$

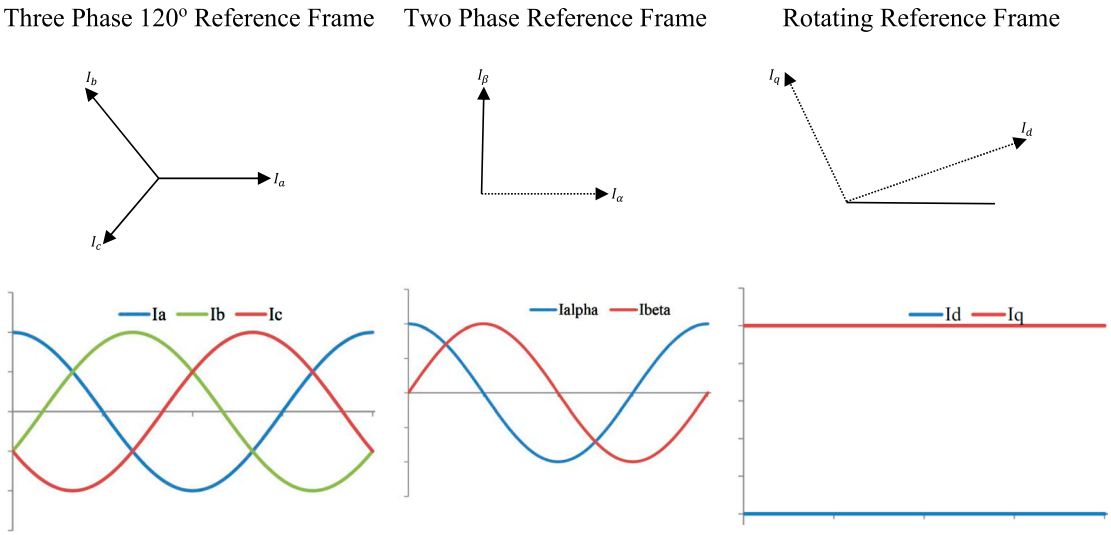

Figure 2. Three reference frames.

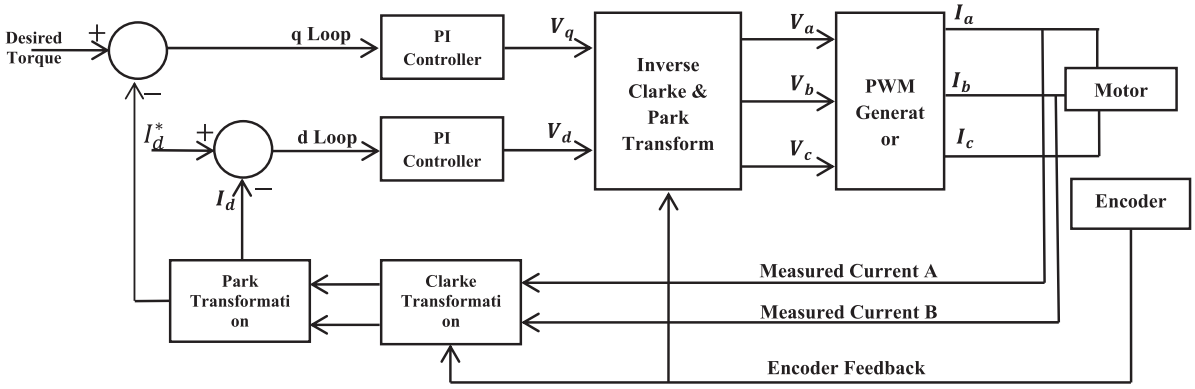

Figure 3. Block diagram of FOC.

$$\varphi_q = L_{sq}.I_{sq} \tag{4}$$

Torque derivation:

$$T_e = \frac{3}{2} n_p.[\varphi_f.I_{sq} + (L_{sd} - L_{sq}).I_{sd}.I_{sq}] \tag{5}$$

The formula above can be rewritten as follows for the surface permanent magnet synchronous motor (SPMSM) since L_{sd} equals L_{sq}.

$$T_e = \frac{3}{2} n_p.\varphi_f.I_{sq} \tag{6}$$

Within the aforementioned formulas, φ_{sd} and φ_{sq} signify the dq axis constituent of stator flux, L_{sd} and L_{sq} denoted dq axis equivalent inductance of stator windings, I_{sd} and I_{sq} signify the dq axis constituent of stator current, ud and uq signify the d and q axis constituent of stator voltage, φ_f represents the PMSM flux, R indicates the stator windings resistance, and ω expresses the rotor speed. Te is proportional toI_{sq}, p indicates differentiation condition, and n_p represents the count of the pole pairs.

Motion derivation:

$$T_e = J * p\left(\frac{\omega}{n_p}\right) + R_\Omega * \frac{\omega}{n_p} + T_L \tag{7}$$

Here, J stands for inertia of rotational force, ω for electrical velocity rotor angular, and TL for load torque. RΩ is the damping coefficient. The current (I_{sq}) is only the torque component in torque function, which is higher when id equal to zero. This is reflected in formula (6), which represents vector control approach, where $I_{sd} = 0$.

4. PMSM FOC control

The efficiency of AC drives is increased by vector control (VC), which was developed at the start of the 1970s and shown in an induction motor that may be controlled by a separately excited DC motor [19]. The instantaneous positions of the voltage, current, and flux space vectors are controlled in VC, which ideally provides the right orientation during transients

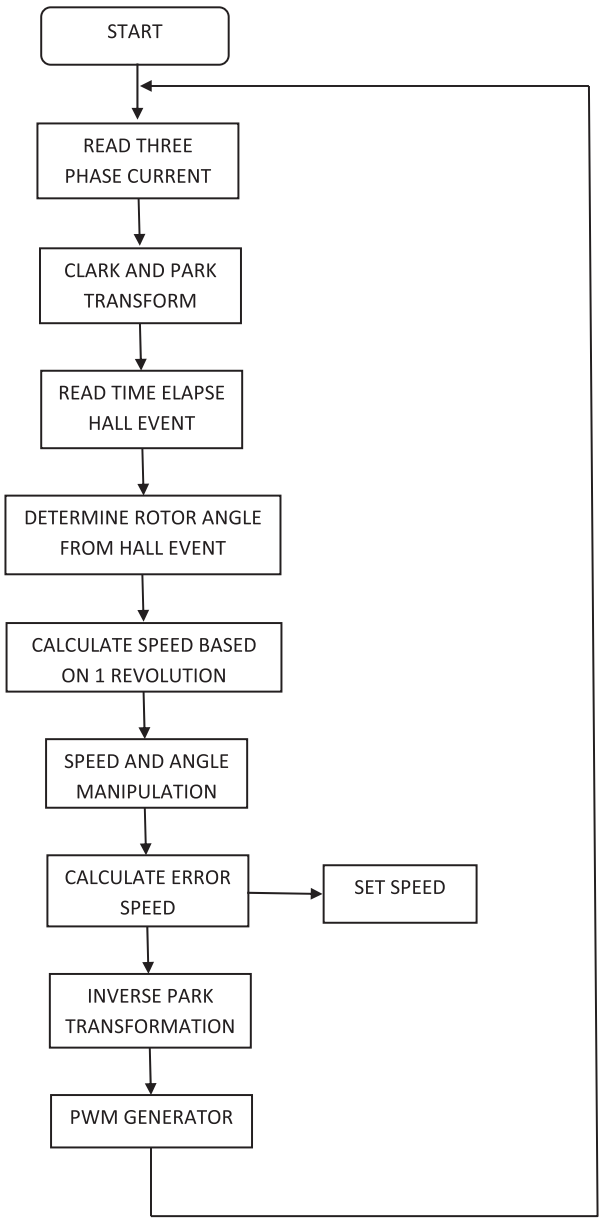

Figure 4. Flow chart of foc controller PMSM drive.

as well as steady states. Both synchronous and asynchronous motor drives can use vector control. There are several similarities between Sinusoidal Control and

Table 3. Rated data of the simulated and tested PMSM motor.

Rated Speeds	1500 rpm
Torques	3.5 Nm
Rated frequencies	50 Hz
Rated Voltages	93 V
Stator resistances	2.8 ohm
Stator Inductances	1.5 mH
Torque Constants	1.05 Nm/A
Pole pairs	4

the Field Oriented Control algorithm. It can, however, attain greater efficiency at high speeds due to a few key distinctions. The primary disadvantage of Sinusoidal Control is that it attempts to regulate motor currents, which direction and magnitude change with time. The PI controllers' limited bandwidth prevents them from handling the operation as the speed and frequency rise. By expressing and managing the current space vector in the two-axis d-q frame of reference, this issue can be solved.

Even though changing current alone seems like the most obvious solution at first, creating variation in torque with a PMSM motor is more challenging. When current is introduced into the rotor perpendicular to the magnetic field, torque is produced. The majority of permanent magnet DC motors use FOC. To apply torque to rotor's position, magnetic field's phase and to motor shaft must be known. In order to compare Hall Effect sensors to vector control, this article will examine them.

Synchronous inductances L_s and their corresponding armature fluxes φ_a are minimal i.e. $\varphi_a = \varphi_m = \varphi_f$. Torque expression outcomes can be represented as Equation 1.

$$T_e = \frac{3}{2} n_p . \varphi_f . I_{sq} \tag{8}$$

Which implies torques is proportional to I_{sq} power factor angles φ equal torque angles δ as depicted in Equation 2.2

$$\cos \emptyset = \varphi_s / \cos \delta = \varphi_f \tag{9}$$

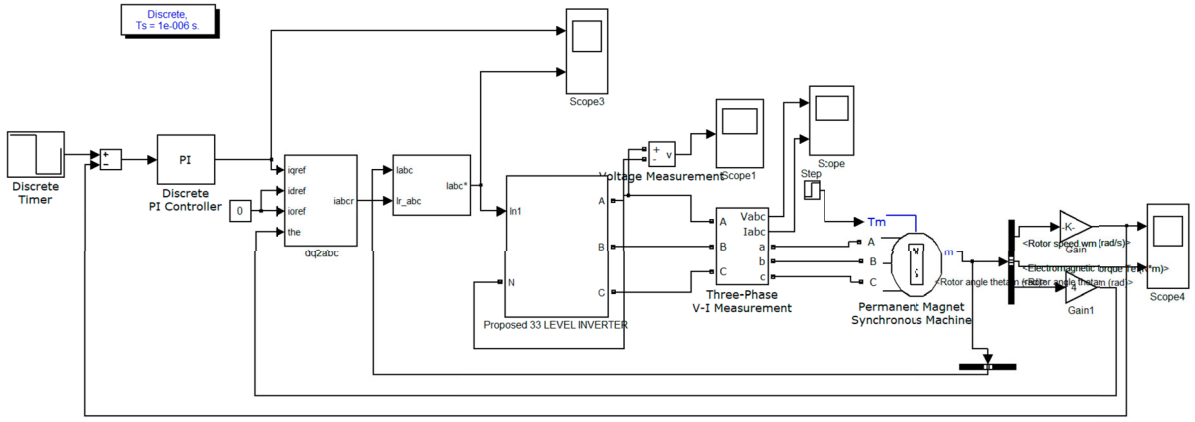

Figure 5. MATLAB simulation model of proposed stacked MLIs based PMSM.

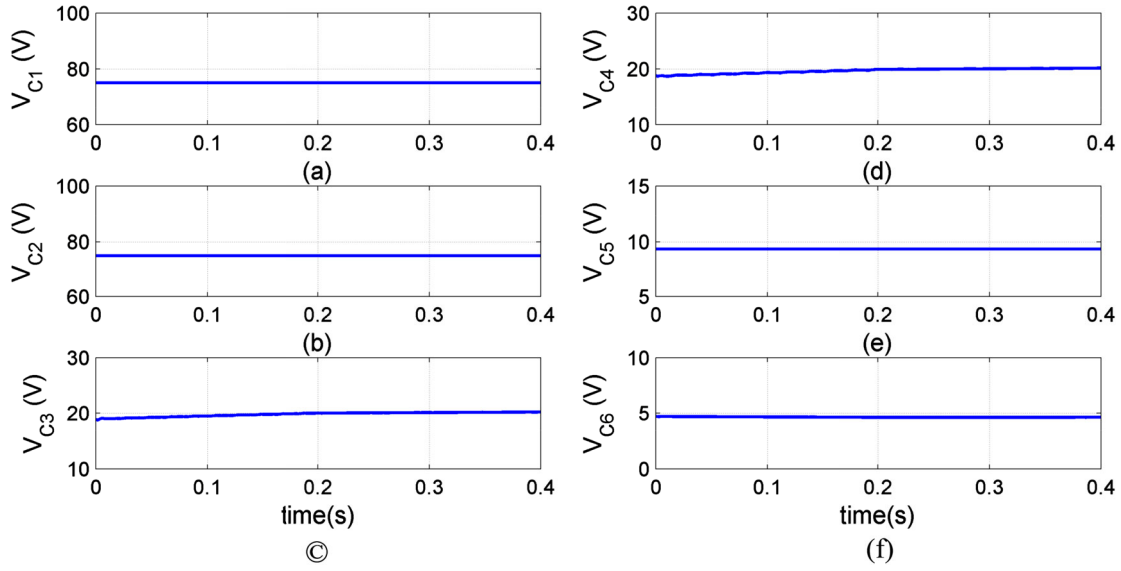

Figure 6. Capacitor voltage of proposed inverter in case.1.

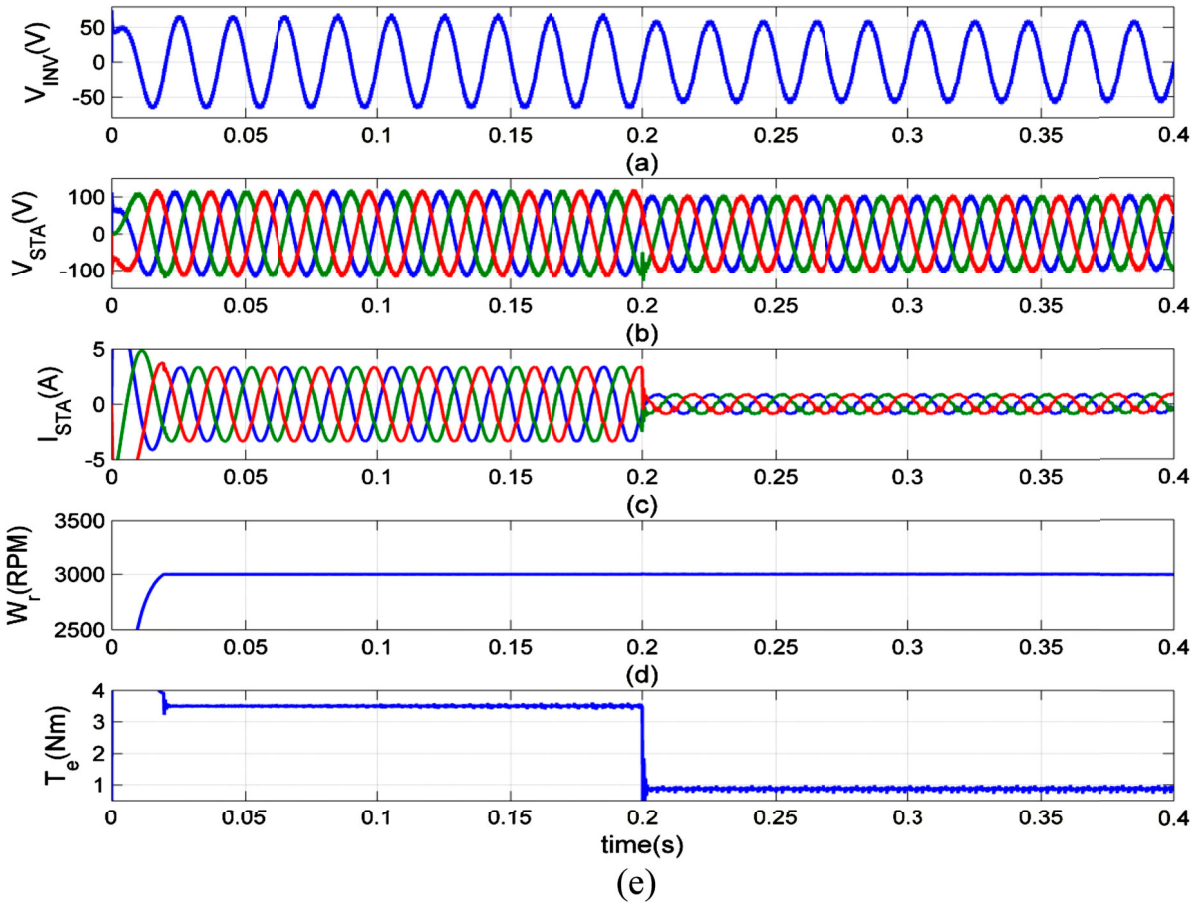

Figure 7. Simulation wave form of proposed stacked MLIS based PMSM in Case.1.

Stator command currents are derived from speed control loops.

FOC (Field Orientation Control) entails controlling the stator current, represented by vectors [20–22]. These controls are developed from projections, which change three-phase systems with time dependence into two-coordinate systems which is time independence (d, q coordinates). These projections result in structures resembling controllers for DC machines. The foundations of control approaches are Clarke and inverse

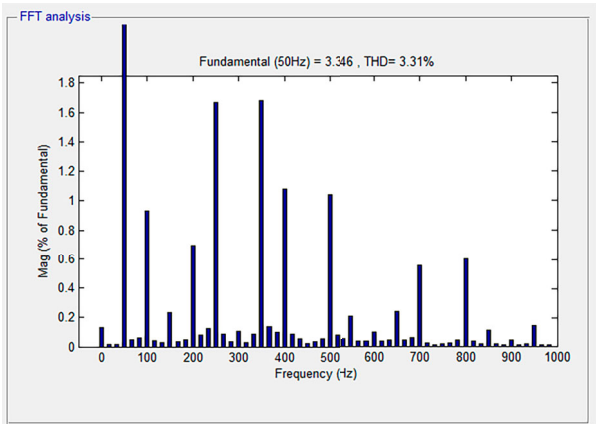

Figure 8. Current THD of proposed inverter in 3.5 Nm case.1.

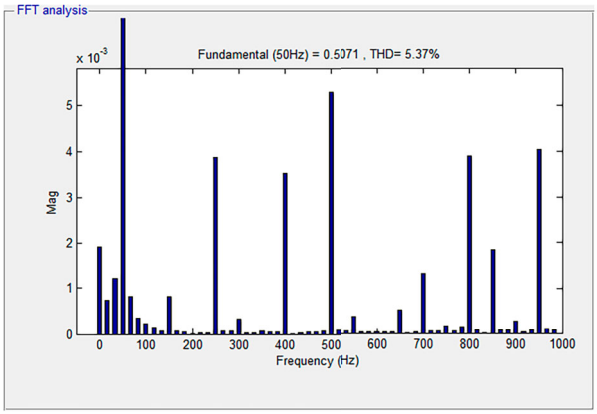

Figure 9. Current THD of proposed inverter in 0.875 Nm case.1.

transformations. The rotating frames of the rotors may be created from the stator's (3Φ) currents. Clarke transformations transform three phase values from three phase frames of references into dual axis orthogonal stable frames of references. Values are never in a fixed frame since the rotor frame rotates continually. The three-phase values are transformed by the Park transformation into an orthogonally oriented frame of reference (direct axis + quadratic axis). Figure 2 displays the three repositories.

The joined Clarke and Park Transformations can be depicted in a Matrix form as:

$$\begin{bmatrix} I_d \\ I_q \end{bmatrix} = \frac{2}{3} \begin{bmatrix} \cos(\theta) & \cos\left(\theta - \frac{2\pi}{3}\right) & \cos\left(\theta + \frac{2\pi}{3}\right) \\ \sin(\theta) & \sin\left(\theta - \frac{2\pi}{3}\right) & \sin\left(\theta + \frac{2\pi}{3}\right) \end{bmatrix} \times \begin{bmatrix} I_a \\ I_b \\ I_c \end{bmatrix} \tag{10}$$

Where I_d and I_q are direct and quadrature axis respectively, θ stands for angular positions of rotors. Similarly, inverse transformations are given by:

$$\begin{bmatrix} I_a \\ I_b \\ I_c \end{bmatrix} = \frac{2}{3} \begin{bmatrix} \cos(\theta) & -\sin(\theta) \\ \cos\left(\theta - \frac{2\pi}{3}\right) & -\sin\left(\theta - \frac{2\pi}{3}\right) \\ \cos\left(\theta + \frac{2\pi}{3}\right) & -\sin\left(\theta + \frac{2\pi}{3}\right) \end{bmatrix} \times \begin{bmatrix} I_d \\ I_q \end{bmatrix} \tag{11}$$

Rotation torque is produced by the quadrature axis component, not the direct axis component, which yields insignificant torque. Optimally, the direction and magnitude of the current space vector in the d-q frame are fixed in relation to the rotor, regardless of rotation. The d-q frame of reference's static current space vector forces the PI controllers to work with DC values instead of sinusoidal signals, significantly streamlining the control structure. The controller frequency response and phase shift on motor torque and speed are thus no longer limited since this isolates the controllers from the time-variant winding currents and voltages.

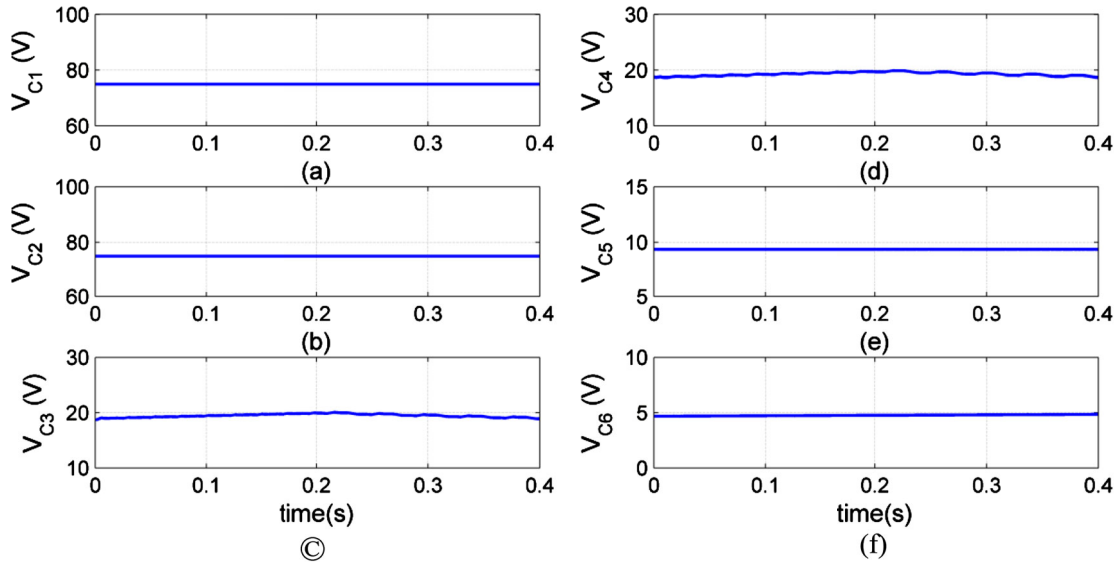

Figure 10. Capacitor voltage of proposed inverter in case.2.

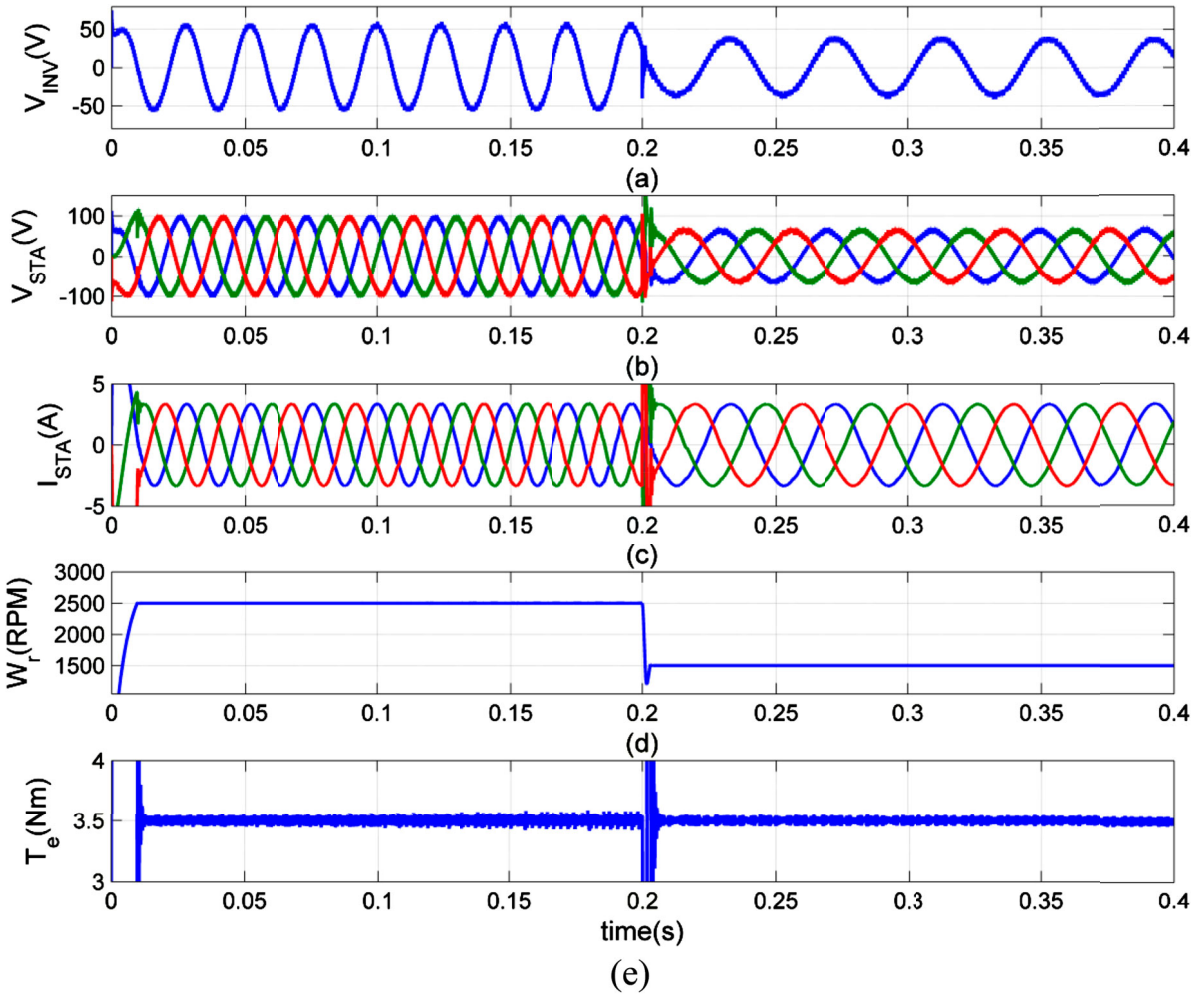

Figure 11. Simulation wave form of proposed stacked MLIS based PMSM in case.2.

Several benefits are possible with the FOC algorithm because it isolates the PI controllers from time-varying currents and voltages. Figures 3 and 4. Shows the block diagram and Flow chart of a typical FOC controller respectively.

FOC algorithm offers multiple benefits, including:

- High efficiency, by shielding the PI controller from time-varying currents and voltages.
- Smooth functioning across a wide speed range, both at low and high speeds.
- Fast dynamic response and good transient and steady performance;
- Convert complicated AC model and coupling into a simple linear system.

The only drawback to the application of FOC is the computationally expensive and challenging nature of the changes that must be completed.

5. Simulation result

For the validation of the previously discussed control approach, simulations on a 33-level STACKED MLI inverter-fed PMSM motor have been carried out using

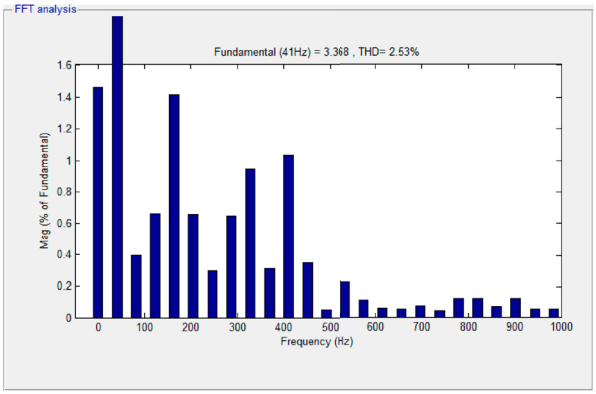

Figure 12. Current THD of proposed inverter in 2500 rpm case.2.

Matlab–Simulink. The simulated PMSM motor ratings are given Table 3. Below. Then the proposed method effectiveness is analyzed by comparing the different technique and different case studies, i.e. case 1 and case 2 (Figures 5 and 6).

Case 1.

This section details the testing of the proposed 33-level PMSM motor drive performance, which is compared by rating the constant speed of 3000 rpm and altering

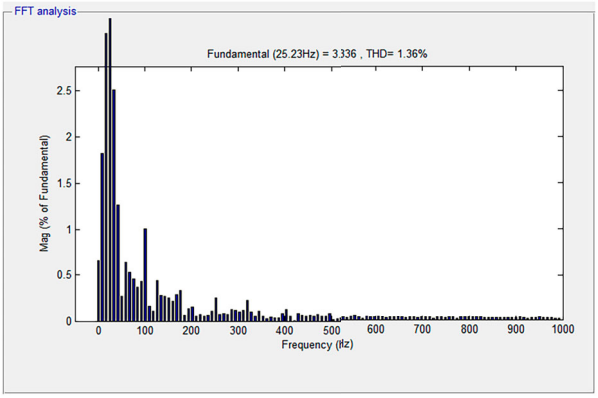

Figure 13. Current THD of proposed inverter in 1500 rpm case.2.

the motor's torque from fully loaded to 25% loaded, or 0.875 Nm. The torque at which the load is applied is expressed as a step, changing from 3.5 Nm to 0.875 Nm in 0.2 s. Figure 4 demonstrates how the voltages of the capacitors $V_{C1}, V_{C2}, V_{C3}, V_{C4}, V_{C5} and V_{C6}$ progressively approach the required value. Figure 7(a)–(c) show the filtered three-phase stator voltage of the PMSM, which is disturbed by the presence of stator inductance. Figure 7(a) displays the output phase voltage of the 31-stage inverter. Figure 7(e) displays the motor's output electromagnetic torque; the engine speed is unaffected by the PMSM vector velocity control as shown in 7(d) as the torque changes from 3.5–0.875 Nm in 0.2 s.

Case 2.

In order to examine the drive performance of the planned 33-level PMSM motor, this section explains how the motor's torque was varied from fully loaded to 25% loaded, or 0.875 Nm, at a ratted constant speed of 3000 rpm. Step changes of the load torque from 3.5 Nm to 0.875 Nm are given in 0.2 s Figure 8 demonstrates how capacitors $V_{C1}, V_{C2}, V_{C3}, V_{C4}, V_{C5}$ *and* V_{C6} voltages self-balance to attain the target value linearly(Figures 9 and 10). Figures 11(b) and (c) display the filtered three-phase stator voltage of the PMSM, which is disturbed by the presence of stator inductance. Figure 11(a) depicts the output phase voltage of the 31-level inverter. Figure 11(d) depicts the PMSM motor's rotor speed. Due to PMSM vector speed controls, but motor torques, the shift from 2500 to 1500 rpm is accomplished in 0.2 s. muscles do not alter, as seen in Figure 11(d).

6. Conclusion

This work proposes a new stacked multilevel inverter topology for symmetric 3-phase PMSM drives, with a single DC supply. The 3-phase stacked multilevel inverter design with two DC sources for a FOC-based PMSM drive is originally described in this work. Next, it suggests a straightforward and innovative way to run the three-phase stacked MLI using a single DC supply. Compared to conventional similar topologies, the suggested topology minimizes the number of power switches, diodes, total blocked voltage, system size, and cost. Lastly, the efficiency and performance of the 33-level STACKED MLI topology with PMSM drive that has been suggested. The results demonstrate that the PMSM power train with FOC provided adequate performance in both simulations with only minor ripple in torque and THD values for thirty three-stage inverter as shown in Table 4. This showed how the high handling capacity and high efficiency of these motors eliminate torque ripples caused by commutation and produce smooth torque with low transient voltage, which improving the PMSM control's performance and reliability in electrical vehicles.

Table 4. Torque ripple comparison of proposed inverter for various conditions.

	Condition		THD (%)	Torque Ripple (Nm)	Torque Ripple (%)
Case 1	3000 RPM	3.5 Nm	3.31%	0.19 Nm	5.74%
		0.875 Nm	5.37%	0.072 Nm	8.22%
Case 1	2500 RPM	3.5 Nm	2.53%	0.12 Nm	3.45%
	1500 RPM		1.36%	0.08 Nm	2.28%

Disclosure statement

No potential conflict of interest was reported by the author(s).

ORCID

N. Subha Lakshmi http://orcid.org/0000-0002-2097-0907

References

[1] Sri hari karthik, India. Available: https://circuitdigest.com/article/different-types-of-motors-used-in-electric-vehicles-ev.

[2] Lulhe AM, Oate TN. A technology review paper for drives used in electrical vehicle (EV) & Hybrid Electrical Vehicles (HEV). 2015 IEEE Conference Proceedings of International Conference on Control, Instrumentation, Communication and Computational Technologies (lCCICCT); 2015. pp. 632–636.

[3] Park S-Z, Kim Y-K, Song C-H, et al. Operation method of electric bicycle using change of BLDC operation mode and PMSM operation mode. IEEE Conference Proceedings of 8th International Conference on Power Electronics; 2011. pp.2529-2536.

[4] Kocabiyik H, Oner Y, Ersoz M, et al. Analysis of Permanent Magnet Synchronous Motor by Different Control Methods with Ansys Maxwell and Simplorer Co-simulation. Proceedings of the International Conference on Artificial Intelligence and Applied Mathematics in Engineering; 2020, pp. 518–525. doi:10.1007/978-3-030-36178-5_41

[5] Pindoriya RM, Rajpurohit BS, Kumar R, et al. Comparative analysis of permanent magnet motors and switched reluctance motors capabilities for electric and hybrid electric vehicles, IEEE; 2018. doi:10.1109/ETECHNXT.2018.8385282

[6] Sheshadri SR, Samanta B. Comparative analysis of IM/BLDC/PMSM drives for electric vehicle traction applications using ANN-based FOC. IEEE Conference Proceedings on 2020 IEEE 17th India Council International Conference; 2020.
[7] Janardanan EG. "Permanent magnet DC motor and brushless permanent magnet DC motor", in special electrical machines. 4th ed. New Delhi: PHI Learning Pvt. Ltd.; 2017, pp.61–63.
[8] Sakunthala S, Kiranmayi R, Nagaraju Mandadi P. A study on industrial motor drives comparison and applications of PMSM and BLDC motor drives. IEEE Conference Proceedings on International Conference on Energy, Communication, Data Analytics and Soft Computing (ICECDS-2017); 2017. doi:10.1109/ICECDS.2017.8390224
[9] Cho Y, Lee K-B, Song JH, et al. Torque-Ripple minimization and fast dynamic scheme for torque predictive control of permanent-magnet synchronous motors, IEEE Transaction on Power Electronics, Vol 30, No.4; 2015. pp. 2182-2190. doi:10.1109/TPEL.2014.2326192.
[10] Qi F, Scharfenstein D, Weiss C, et al. Motor Handbook, "Infineon Technologies AG together with Institute for Power Electronics and Electrical Drives, RWTH Aachen University/ Germany. Version: 2.1, Release Date: 12.03.2019, pp 47–51. Available from: https://www.infineon.com/dgdl/Infineon-motor control handbook Additional Technical Information - v01_00-N.pdf? file Id = 5546d4626bb628d7016be6a9aa637e69.
[11] Azam AFN, Jidin A, Ngatiman NA, et al. Current Control of BLDC Drives for EV Application, 2013 IEEE conference proceedings of 7th international power engineering and optimization conference (PEOCO 2013), Langkawi, Malaysia; 2013, pp.411-416.
[12] Sawhney AK. A Course in Electrical Machine Design, Dhanpat Rai and Co publication, New Delhi, Edition; 2016.
[13] Manual on "Design and Finite Element Analysis of Induction Machines using ANSYS RMxprt, Maxwell 2D & 3D Design", Entuple Technologies, Bangalore, India.
[14] Yongjuan C, Qiang L, Li Y. A software for design and analysis of PMSM based on ANSYS. Proceedings of The 1st International Conference on Information Science and Engineering (ICISE2009); 2009.
[15] Kachin OS, Kiselev AV, Serov AB. Research of operation modes of the synchronous electric motor drive system with Use of software ANSYS Maxwell and simplorer, Proceedings of 15th International Conference On Micro/Nanotechnologies And Electron Devices Edm; 2014.
[16] HBK. https://evreporter.com/motor-controllers-in-evs-india-relying-on-imports/
[17] Sundaram M, Anand M, Chelladurai J, et al. Design and FEM Analysis of High-Torque Power Density Permanent Magnet Synchronous Motor (PMSM) for Two-Wheeler E-Vehicle Applications",International Transactions on Electrical Energy Systems; 2022, pp.1-14.
[18] Bdewi MY, Mohammed AM, Ezzaldean MM. Design and performance analysis of permanent magnet synchronous motor for electric vehicles application. Engineering and Technology Journal; 39(3):394–406.
[19] ManelFitouri Y, NaceurAbdelkrim M. Analysis and Co-simulation of permanent magnet sychronous motor with short-circuit fault by finite element method. IEEE Xplore Conference Proceedings On System, Signals and Devices; 2016, pp. 472–477.
[20] NamithaMurali S, Ushakumar Mini VP. "Performance comparison between different rotor configuration of PMSM for EV application", IEEE Xplore Conference Proceedings TENCON; 2020, pp.1334-1339.
[21] Sano H, Schneider N, Tani K, et al. Finite Element Analysis of a VR Resolver.
[22] Considering the Mesh Density and the Leakage Flux from a PMSM. IEEE Xplore Conference Proceedings on Electrical Machines (ICEM); 2020, pp. 2520-2526.
[23] Dwivedi S, Singh B. Vector Control vs Direct Torque Control comparative evaluation for PMSM drive, 2010 Joint international conference on power electronics, drives and energy systems & 2010 Power India, New Delhi; 2010, pp. 1-8.
[24] Lin H, Chen S, Yao J, et al. Sensorless vector control system of permanent magnet synchronous motors based on adaptive and fuzzy control. International Conference on Electrical Machines and Systems; 2008, pp. 3074-3078.
[25] S.S. Sivaraju, J. Chitra, T. Anuradha, and A. Pandian, An Intelligent load balancing strategy for energy cost minimization in EV applications", Electric Power Components and System; 2023. doi:10.1080/15325008.2023.2239217.